Solid Freeform Fabrication 2024: Proceedings of the 35th Annual International Solid Freeform Fabrication Symposium – An Additive Manufacturing Conference
Reviewed Paper

Comparative Analysis of Mechanical and Electrical Properties of 3D Printing Carbon Nanotube-Reinforced Materials

[1]Shamil Gudavasov, [2]Ismail Fidan, [1]Mohammad Alshaikh Ali, [1]Vivekanand Naikwadi, [1]Mushfig Mahmudov, [1]Elijah Hudson

[1]Department of Mechanical Engineering, College of Engineering
Tennessee Tech University, Cookeville, TN 38505, USA

[2]Department of Manufacturing and Engineering Technology, College of Engineering
Tennessee Tech University, Cookeville, TN 38505, USA

Abstract

Manufacturing nanocomposite materials through the Material Extrusion (ME) process opens up new possibilities for industries demanding materials with superior conductivity and mechanical robustness. Furthermore, the electrical and mechanical properties of the thermoplastic materials can be increased by the addition of nanofillers, like carbon nanotubes (CNTs). This study aims to compare the mechanical and electrical properties of 3D printed specimens using three different polymers: CNT-reinforced Polylactic Acid (CNT-PLA), CNT-reinforced Acrylonitrile Butadiene Styrene (CNT-ABS), and CNT-reinforced Polyethylene Terephthalate Glycol (CNT-PETG). Tensile specimens are fabricated under varying parameters, including nozzle temperature, nozzle size, printing orientation, and layer thickness. Tensile testing is conducted to investigate the mechanical performance and volume resistivity is utilized to investigate electrical behavior. By understanding the relationship between CNT reinforcement and material properties, this research could pave the way for the development of advanced materials with customized mechanical and electrical characteristics, suitable for a wide range of industrial applications.

1. Introduction

CNT-reinforced polymers have attracted increasing attention due to their remarkable ability to enhance the mechanical and electrical properties of thermoplastics such as PLA, ABS, and PETG. The addition of CNTs into these materials has led to significant improvements in strength, conductivity, and durability, making them ideal for applications in fields like aerospace, automotive, biomedical devices, and electronics. In particular, CNT-reinforced polymers can optimize material performance in 3D printing, where precise control over material properties is crucial. By adjusting parameters such as nozzle temperature, layer thickness, and print orientation, it is possible to achieve tailored characteristics in 3D-printed parts, enabling their use in a wide range of demanding applications [1, 2].

The incorporation of CNTs into polymers has garnered significant interest due to the exceptional mechanical, electrical, and thermal properties of CNTs [3]. These properties can dramatically improve the performance of polymer-based materials, making CNT-reinforced polymers ideal for advanced applications [4]. The addition of CNTs to thermoplastics like PLA, ABS, and PETG can enhance their mechanical strength, electrical conductivity, and thermal stability. Several critical reviews have highlighted the importance of utilizing the CNTs in the ME process to improve the quality and performance of 3D-printed parts [5–10].

The integration of thermoplastics and thermosets with reinforcing fibers, such as short carbon fibers (SCFs) and CNTs, has been shown to significantly improve their mechanical and thermal properties. While SCFs are micrometer-scale fibers that primarily enhance the tensile strength and stiffness of composites, CNTs are nanoscale tubes that not only reinforce mechanical properties but also significantly improve electrical and thermal conductivity due to their unique structure and high aspect ratio. A comprehensive review has highlighted various breakthroughs in materials and ME technologies, their integration with emerging technologies, and the impact of ME across multiple sectors [11]. Fatigue analysis of these materials highlights the impact of varying process parameters on the fatigue life and performance of the composites [12, 13].

ME is a versatile and widely used 3D printing process that enables the fabrication of complex geometries with precise control over material deposition. By integrating CNTs into thermoplastic matrices and utilizing ME, it is possible to produce functionally graded nanocomposite materials with superior properties [14].

This study aims to compare the mechanical and electrical properties of 3D-printed specimens using CNT-reinforced PLA, ABS, and PETG. The specimens are fabricated under varying parameters, including nozzle temperature, nozzle size, printing orientation, and layer thickness. Tensile testing is conducted to investigate the mechanical properties, while volume resistivity measurements are used to evaluate the electrical properties. Understanding the relationship between CNT reinforcement and material properties will provide insights into the development of advanced materials with customized characteristics for a wide range of industrial applications. Although challenges such as achieving uniform CNT dispersion and integrating CNTs with distinct materials, for example, with functionally graded materials persist, highlighting the need for innovation to fully leverage the advantages of enhanced mechanical, electrical, and thermal properties. [15–20].

2. Materials and Methods

2.1. Materials Selection

The selection of materials for this study was guided by their compatibility with 3D printing processes and their potential for enhancement through CNT reinforcement. Three thermoplastic polymers were chosen: PLA, ABS, and PETG. These materials were selected based on their distinct mechanical and electrical properties, making them suitable for a comparative analysis of the effects of CNT reinforcement.

PLA is a biodegradable thermoplastic derived from renewable resources such as corn starch or sugarcane. The CNT-PLA used in this study is 3DXSTAT™ ESD-PLA, an advanced ESD-safe compound designed for critical applications requiring electrostatic discharge (ESD) protection. This material offers consistent surface resistance in the range of 10^7 to 10^9 ohms, making it ideal for applications in the semiconductor and industrial sectors. It also provides improved mechanical properties such as enhanced impact resistance and elongation retention, along with environmental benefits like being biodegradable and having low odor emissions. The recommended printing parameters for 3DXSTAT™ ESD-PLA include an extruder temperature of 210-240°C and a bed temperature of 23-60°C, with drying instructions of 65°C for 4 hours before printing.

ABS is a petroleum-based thermoplastic known for its toughness, impact resistance, and ease of machining. The CNT-ABS used in this study is 3DXSTAT™ ESD-ABS, which is designed for critical applications requiring ESD protection and a high level of cleanliness. ABS is known for its high thermal stability, making it suitable for industrial-grade parts. The recommended printing parameters for 3DXSTAT™ ESD-ABS are an extruder temperature of 220-240°C and a bed temperature of 100-110°C, with drying instructions of 80°C for 4 hours before printing.

PETG is a modified version of Polyethylene Terephthalate (PET), offering a balance between the mechanical properties of PLA and the toughness of ABS. The CNT-PETG used in this study is 3DXSTAT™ ESD-PETG, designed for critical applications requiring ESD protection. It also features superior chemical resistance and low moisture absorption, reducing the risk of printing defects. The recommended printing parameters for 3DXSTAT™ ESD-PETG include an extruder temperature of 230-260°C and a bed temperature of 60-90°C, with drying instructions of 65°C for 4 hours before printing.

All three materials were chosen for their specific properties that cater to different industrial applications requiring ESD protection. The CNT reinforcement is expected to enhance their mechanical and electrical performance, making them suitable for use in various high-performance applications, including semiconductor components and industrial equipment.

2.2. Methodology

2.2.1. 3D Printing Parameters

The fabrication of tensile specimens using CNT-PLA, CNT-ABS, and CNT-PETG was conducted through ME process. Tensile test specimens were printed according to ASTM D638 standards. The specimens were designed in a dumbbell shape to ensure a uniform distribution of stress during testing [21]. Specimen sample is shown in Figure 1.

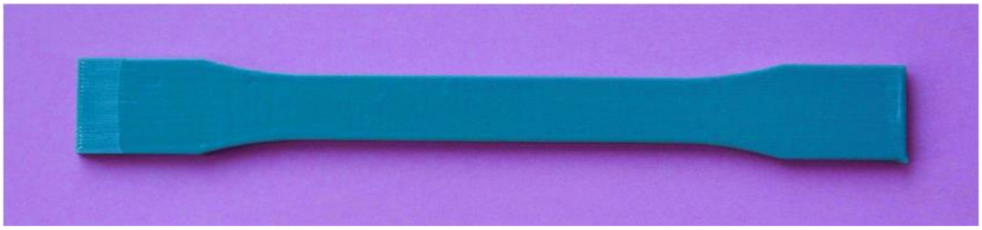

Figure 1. Demonstration of specimen before Tensile testing.

To ensure reproducibility and thoroughly investigate the effects on the mechanical and electrical properties of the printed parts, the 3D printing parameters were meticulously controlled. The nozzle temperature, crucial for optimal material flow and proper layer adhesion, was set according to manufacturer recommendations and previous studies. Bed temperature was adjusted to prevent warping and improve first-layer adhesion, with higher settings benefiting ABS due to its higher melting point. Nozzle size, determining extrusion width, influenced resolution and mechanical properties, and was varied for impact analysis. Printing orientation, affecting tensile strength, was tested in both XY and XZ orientations to study anisotropic behavior. Layer thickness, influencing resolution and mechanical properties, was varied to optimize results. The parameters are detailed in Table 1, providing a comprehensive approach that ensured detailed analysis of each parameter's impact on the printed specimens' performance.

Table 1. 3D printing parameters for CNT-PLA, CNT-ABS, and CNT-PETG

Parameter	ESD-PLA	ESD-PETG	ESD-ABS
Nozzle Temperature	210-220°C	230-260°C	210-220°C
Bed Temperature	60°C	75°C	90°C
Nozzle Size	0.4-0.8 mm	0.4-0.8 mm	0.4-0.8 mm
Orientation	XY-XZ	XY-XZ	XY-XZ
Layer Thickness	0.2-0.3 mm	0.2-0.3 mm	0.2-0.3 mm

2.2.2. Design of Experiments (DOE)

To systematically study the effects of different 3D printing parameters on the mechanical and electrical properties of CNT-PLA, CNT-ABS, and CNT-PETG, a design of DOE approach was utilized. In Table 2, DOE table details the experimental runs for each material under varying 3D printing parameters. For CNT-PLA, the experiments cover nozzle temperatures T_1 (210°C) and T_2 (220°C), with both XY and XZ orientations tested. For CNT-ABS, the experiments cover nozzle temperatures T_1 (220°C) and T_2 (240°C), with both orientations. For CNT-PETG, the experiments include nozzle temperatures T_1 (230°C) and T_2 (260°C), with both XY and XZ orientations tested. Here, T_1 and T_2 represent the respective temperature ranges for each material.

This table provides a structured overview of the different parameter combinations tested in this study, facilitating a detailed analysis of their impact on the mechanical and electrical properties of the 3D-printed specimens. This comprehensive DOE approach ensures that the study captures the influence of each parameter on the performance of the CNT-reinforced materials, allowing for the optimization of 3D printing conditions to achieve the desired material characteristics.

2.3. Testing Procedures

The testing procedures for this study involved evaluating both the mechanical and electrical properties of the 3D-printed specimens made from CNT-reinforced PLA, ABS, and PETG. The tests were designed to provide a comprehensive understanding of how CNT reinforcement affects these properties.

Table 2. Expanded DOE table

Run	Orientation	Nozzle Diameter	Nozzle Temp.	Layer Thickness
1	XY	0.4	T_1	0.2
2	XY	0.4	T_1	0.3
3	XY	0.4	T_2	0.2
4	XY	0.4	T_2	0.3
5	XY	0.8	T_1	0.2
6	XY	0.8	T_1	0.3
7	XY	0.8	T_2	0.2
8	XY	0.8	T_2	0.3
9	XZ	0.4	T_1	0.2
10	XZ	0.4	T_1	0.3
11	XZ	0.4	T_2	0.2
12	XZ	0.4	T_2	0.3
13	XZ	0.8	T_1	0.2
14	XZ	0.8	T_1	0.3
15	XZ	0.8	T_2	0.2
16	XZ	0.8	T_2	0.3

2.3.1. Tensile Testing

To evaluate the mechanical properties of the 3D-printed specimens, tensile testing was conducted using an Instron tensile testing machine [22, 23]. The key features and components of the machine are outlined below:

Load Frame: The tensile testing machine features a robust load frame capable of accommodating single or dual column configurations, depending on the force capacity required.

Software: The machine is equipped with advanced test software that allows operators to configure test methods and output results efficiently.

Load Cell: A highly accurate load cell is used to measure the force applied to the test specimen. Instron's load cells offer precision down to 1/1000 of their capacity.

Grips and Fixtures: The machine includes a variety of specimen grips and fixtures, designed to accommodate different materials, shapes, and sizes, ensuring versatility in testing.

Strain Measurement: For some test methods, precise measurement of specimen elongation under load is required. Instron's AVE2 system can measure changes in specimen length with an accuracy of ±1 µm or 0.5% of the reading.

The image of the tensile testing machine used in the study is illustrated in Figure 2.

Figure 2. Tensile testing machine

In Figure 3, the image demonstrates the specimen before and after tensile testing. The top part of the image displays the intact specimen before the test, while the bottom part shows the specimen after testing, where it has fractured at its weakest point due to the applied tensile force. This visual illustrates how the tensile test evaluates the material's strength and failure characteristics.

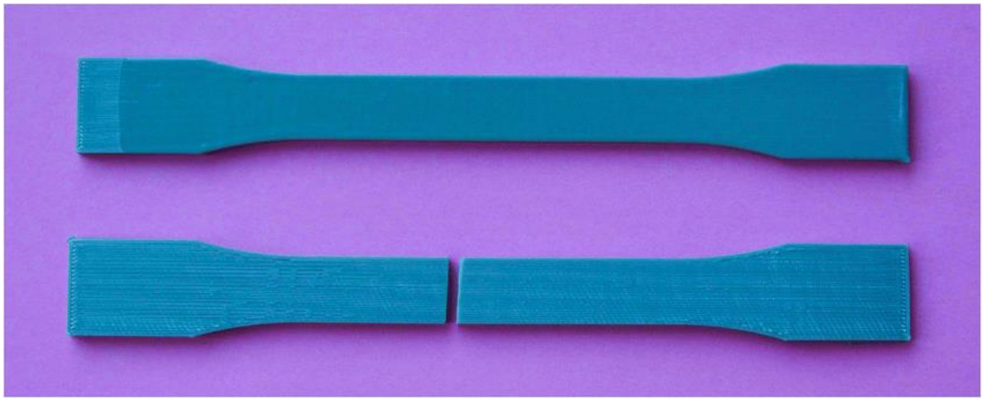

Figure 3. Demonstration of specimen before and after Tensile testing.

2.3.2. Electrical Resistivity

In this study, the electrical conductivity of CNT-reinforced PLA, ABS, and PETG filaments was measured using a structured and controlled methodology. The process involved using a DC power supply, ammeter, and crocodile clip wires to hold the filaments and establish a stable electrical connection. The voltage was increased incrementally, starting from 50V and rising to 350V, with current values recorded at each step. This setup ensured consistent contact and minimal resistance interference, allowing for precise measurement of the electrical properties across the different materials. By maintaining the integrity of the connections, the methodology provided accurate data essential for understanding how the CNT reinforcement affects electrical conductivity in filaments.

The data gathered during the process was used to calculate both volume resistivity and electrical conductivity. Volume resistivity (ρ) was calculated using the formula (1):

$$\rho = R \times \frac{A}{L} \quad (1)$$

where R is resistance, A is the cross-sectional area, and L is the length of the filament. The electrical conductivity (σ), defined as the inverse of resistivity, was determined using the formula (2):

$$\sigma = \frac{I \times L}{V \times A} \quad (2)$$

where I is the current, V is the voltage, L is the filament length, and A is its cross-sectional area. This approach provided crucial insights into the conductive behavior of CNT-reinforced filaments and helped establish their potential use in various applications requiring enhanced electrical performance.

3. Results and Discussion

3.1. Mechanical Properties

The mechanical properties of CNT-reinforced PLA, ABS, and PETG specimens were evaluated through tensile testing. The ultimate tensile strength (UTS) was determined for each material under different printing conditions [24].

3.1.1. CNT-PETG Analysis

As it is given in Figure 4, UTS graph for CNT-PETG shows how different printing parameters influence the material's mechanical performance. The highest UTS, 41.83 MPa, is recorded in Run 7, where an XY orientation, 0.8 mm nozzle diameter, 260°C nozzle temperature, and 0.2 mm layer thickness were used. This indicates that thinner layers and higher nozzle temperatures enhance the tensile strength of CNT-PETG. Comparatively, lower UTS values are seen in Runs 9 and 10 (13.45 MPa and 14.69 MPa, respectively), where a thicker layer of 0.3 mm was used, showing a clear negative impact on strength due to the thicker layers. Overall, the data highlight the importance of optimizing printing parameters to achieve maximum mechanical strength in CNT-PETG.

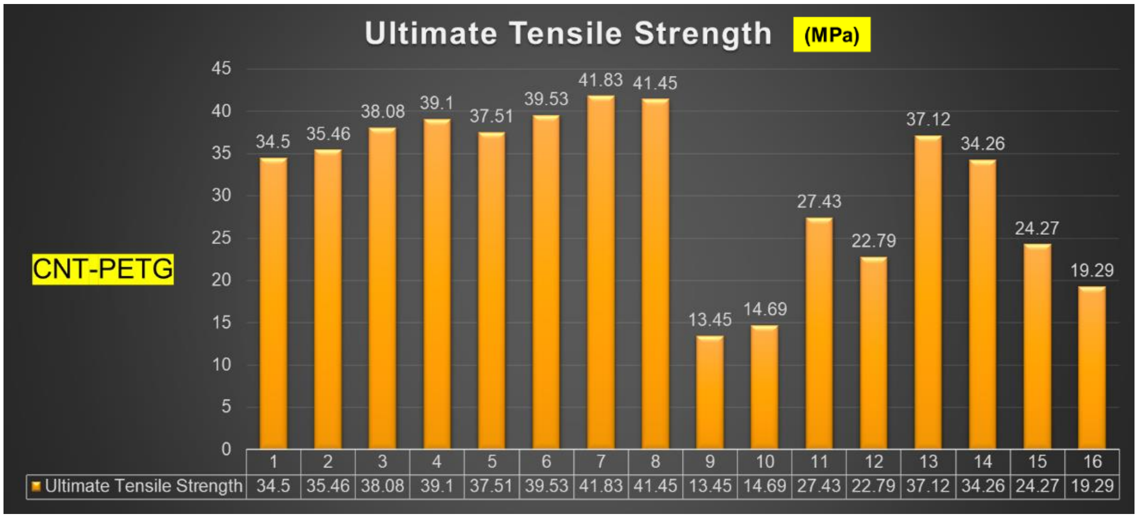

Figure 4. UTS of CNT-PETG with varying printing parameters.

3.1.2. CNT-ABS Analysis

For CNT-ABS, in Figure 5, the UTS graph displays a peak tensile strength of 30.88 MPa in Run 5, achieved with an XY orientation, 0.8 mm nozzle diameter, 220°C nozzle temperature, and 0.2 mm layer thickness. This run suggests that thinner layers and higher nozzle temperatures are beneficial for mechanical performance. However, Runs 9 and 10 show significant drops in tensile strength to 13.73 MPa and 8.5 MPa, respectively, due to thicker layers, indicating that CNT-ABS is particularly sensitive to layer thickness. Despite its lower mechanical performance compared to CNT-PETG and CNT-PLA, CNT-ABS still provides sufficient strength for specific applications, especially when printing parameters are optimized.

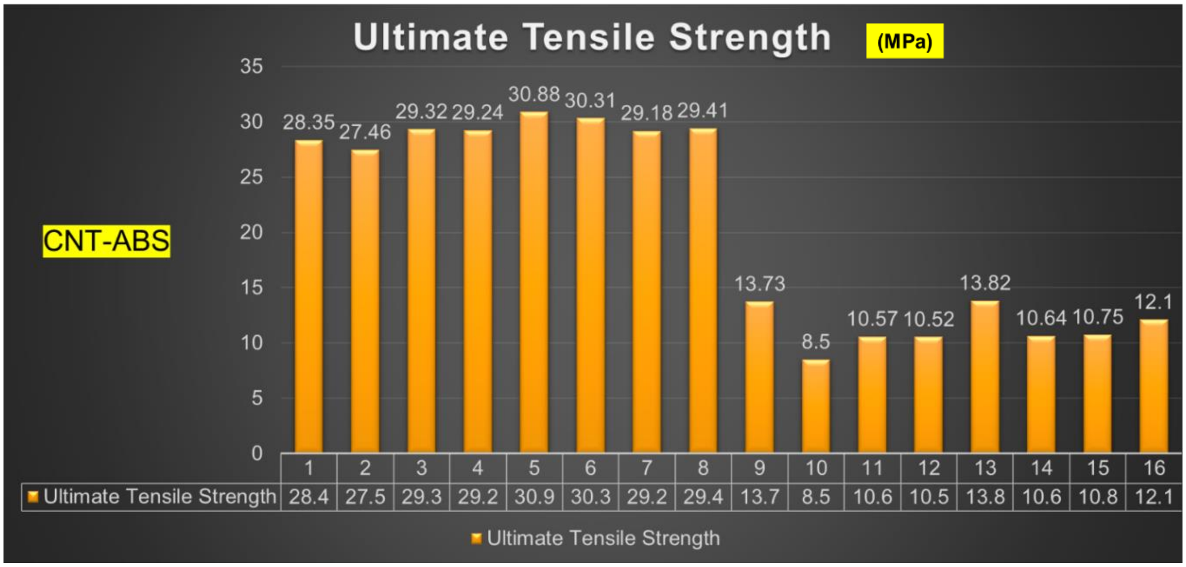

Figure 5. UTS of CNT-ABS with varying printing parameters.

3.1.3. CNT-PLA Analysis

In Figure 6, the CNT-PLA UTS graph reveals the material's superior mechanical properties, with a maximum UTS of 56.16 MPa in Run 8. This high value was achieved with an XY orientation, 0.8 mm nozzle diameter, 220°C nozzle temperature, and 0.3 mm layer thickness. CNT-PLA consistently shows high tensile strength across most runs, with values over 50 MPa in several cases. This indicates that CNT-PLA, even with a slightly thicker layer, maintains excellent mechanical integrity. However, Runs 9 and 10 exhibit a notable decrease in UTS, showing that layer thickness still plays a role, though less significantly compared to other materials. CNT-PLA's high tensile strength makes it ideal for applications requiring structural durability.

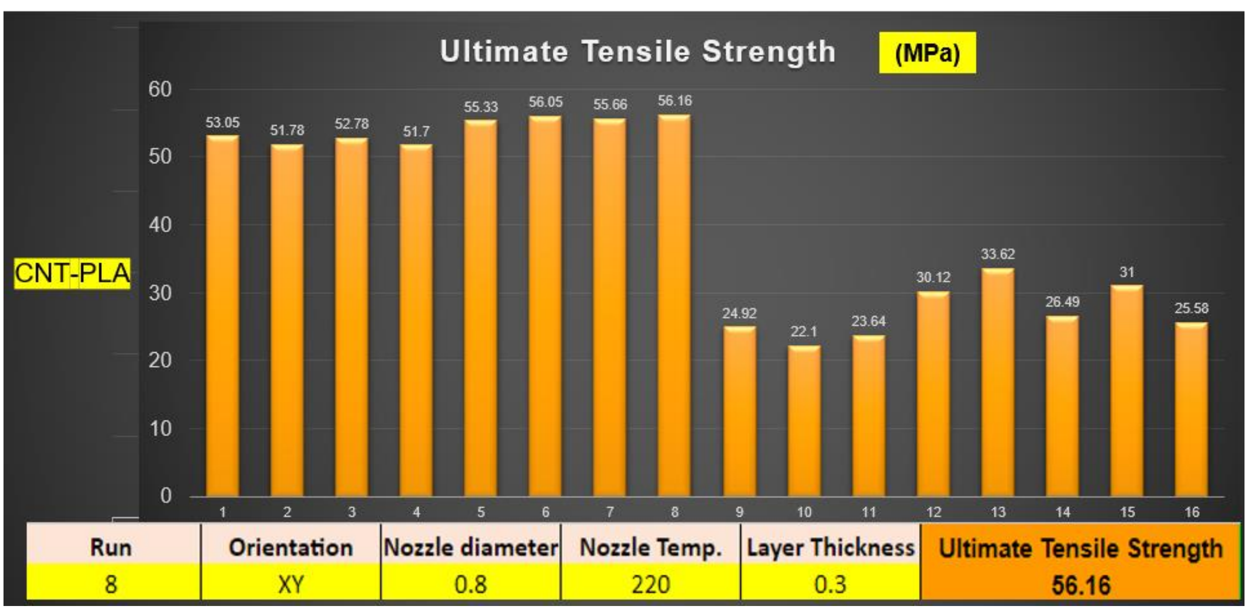

Figure 6. UTS of CNT-PLA with varying printing parameters.

3.2. Electrical Properties

The Voltage-Current Characterization graph for CNT-reinforced filaments shows the relationship between the applied voltage (V) and the resulting current (I) for CNT-ABS, CNT-PETG, and CNT-PLA filaments in Figure 7. As the voltage increases from 50V to 350V, CNT-ABS exhibits the highest current response, reaching 1.84 µA at 350V. CNT-PETG follows, reaching a maximum of 1.25 µA, while CNT-PLA displays the lowest current values, peaking at 0.45 µA.

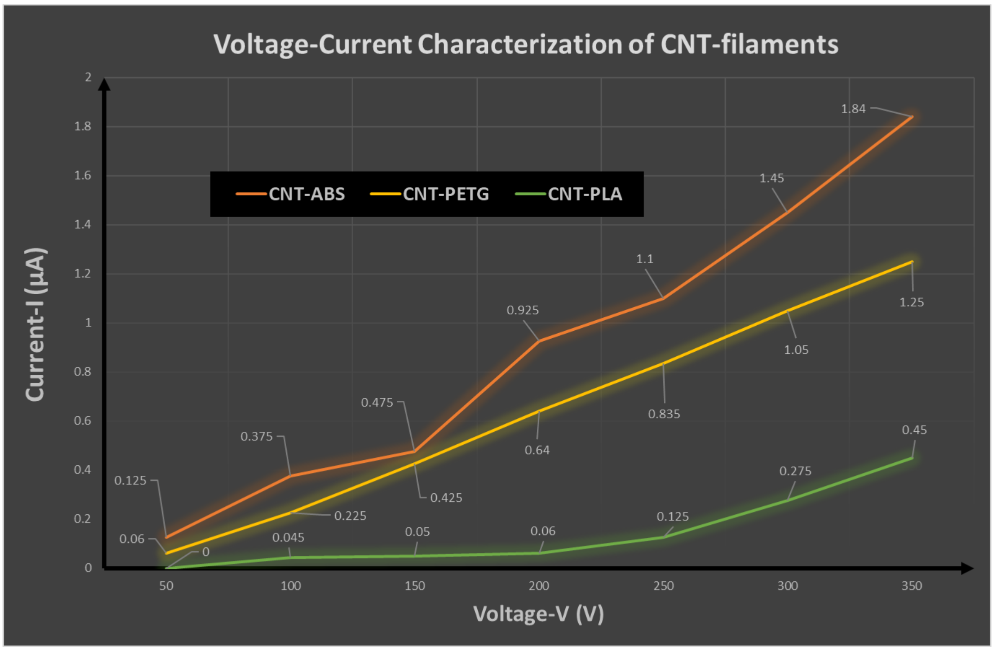

Figure 7. Voltage-Current Characterization of CNT-reinforced filaments.

The graph reveals that CNT-ABS and CNT-PETG show linear trends, with consistent increases in current as the voltage increases. CNT-PLA, however, shows a much more gradual slope, indicating a slower increase in current with voltage. Notably, CNT-ABS demonstrates the steepest rise in current, followed by CNT-PETG and then CNT-PLA. This suggests distinct differences in how each material responds to increasing voltage, with CNT-ABS showing the most pronounced change, and CNT-PLA the least.

4. Conclusions

This study highlights the significant influence of printing parameters on both the mechanical and electrical properties of CNT-reinforced PLA, ABS, and PETG materials. The optimal mechanical performance was observed with higher nozzle temperatures (220°C for PLA and ABS, 260°C for PETG), larger nozzle diameters (0.8 mm), and thinner layer thicknesses (0.2 mm). CNT-PLA demonstrated the highest tensile strength at 56.16 MPa, making it ideal for applications requiring high structural integrity. CNT-PETG achieved a moderate tensile strength of 41.83 MPa, while CNT-ABS, although lower in tensile strength at 30.88 MPa, performed better in terms of electrical conductivity.

In terms of electrical properties, CNT-ABS exhibited the highest current flow, reaching 1.84 µA at 350V, indicating its superior conductive performance. CNT-PETG followed with a maximum current of 1.25 µA, while CNT-PLA showed the lowest current, peaking at 0.45 µA. These results emphasize the trade-off between mechanical and electrical performance, where CNT-PLA excels in mechanical strength, while CNT-ABS is more suitable for applications requiring enhanced electrical conductivity.

Acknowledgements

The support provided by the Center for Manufacturing Research, Department of Mechanical Engineering, and Department of Manufacturing and Engineering Technology is greatly appreciated.

References

1. Alkunte S, Fidan I, Naikwadi V, et al (2024) Advancements and Challenges in Additively Manufactured Functionally Graded Materials: A Comprehensive Review. Journal of Manufacturing and Materials Processing 8:23. https://doi.org/10.3390/jmmp8010023
2. Fidan I, Alshaikh Ali M, Naikwadi V, et al (2024) Nano-Level Additive Manufacturing: Condensed Review of Processes, Materials, and Industrial Applications. Technologies (Basel) 12:117. https://doi.org/10.3390/TECHNOLOGIES12070117
3. Mora A, Verma P, Kumar S (2020) Electrical conductivity of CNT/polymer composites: 3D printing, measurements and modeling. Compos B Eng 183:. https://doi.org/10.1016/j.compositesb.2019.107600
4. Parnian P, D'Amore A (2021) Fabrication of high-performance cnt reinforced polymer composite for additive manufacturing by phase inversion technique. Polymers (Basel) 13:. https://doi.org/10.3390/polym13224007
5. Iqbal A, Saeed A, Ul-Hamid A (2021) A review featuring the fundamentals and advancements of polymer/CNT nanocomposite application in aerospace industry. Polymer Bulletin 78:539–557. https://doi.org/10.1007/S00289-019-03096-0
6. Shaqour B, Abuabiah M, Abdel-Fattah S, et al (2021) Gaining a better understanding of the extrusion process in fused filament fabrication 3D printing: a review. International Journal of Advanced Manufacturing Technology 114:1279–1291. https://doi.org/10.1007/S00170-021-06918-6
7. Kristiawan RB, Imaduddin F, Ariawan D, et al (2021) A review on the fused deposition modeling (FDM) 3D printing: Filament processing, materials, and printing parameters. Open Engineering 11:639–649. https://doi.org/10.1515/ENG-2021-0063

8. Nurazzi NM, Asyraf MRM, Khalina A, et al (2021) Fabrication, Functionalization, and Application of Carbon Nanotube-Reinforced Polymer Composite: An Overview. Polymers 2021, Vol 13, Page 1047 13:1047. https://doi.org/10.3390/POLYM13071047

9. Huseynov O, Patterson AE, Ali MA, et al (2024) Critical review on short fiber-reinforced composite materials manufactured by material extrusion: from thermal perspective. Progress in Additive Manufacturing. https://doi.org/10.1007/S40964-024-00673-2

10. Fidan I, Fidan P, Alkunte SS, et al (2024) Unique Instructional Delivery of Additive Manufacturing: A Holistic Review. 2024 ASEE Annual Conference & Exposition Proceedings. https://doi.org/10.18260/1-2--48204

11. Fidan I, Huseynov O, Ali MA, et al (2023) Recent Inventions in Additive Manufacturing: Holistic Review. Inventions 2023, Vol 8, Page 103 8:103. https://doi.org/10.3390/inventions8040103

12. Rajeshirke M, Alkunte S, Huseynov O, Fidan I (2023) Fatigue analysis of additively manufactured short carbon fiber-reinforced PETG Components. International Journal of Advanced Manufacturing Technology 128:. https://doi.org/10.1007/s00170-023-12107-4

13. Gupta A, Hasanov S, Alifui-Segbaya F, Fidan I (2023) Composites (Fiber-Reinforced Plastic Matrix Composites). Springer Handbooks Part F1592:627–637. https://doi.org/10.1007/978-3-031-20752-5_37

14. Bardot M, Schulz MD (2020) Biodegradable Poly(Lactic Acid) Nanocomposites for Fused Deposition Modeling 3D Printing. Nanomaterials 2020, Vol 10, Page 2567 10:2567. https://doi.org/10.3390/NANO10122567

15. Hasanov S, Alkunte S, Rajeshirke M, et al (2021) Review on Additive Manufacturing of Multi-Material Parts: Progress and Challenges. Journal of Manufacturing and Materials Processing 2022, Vol 6, Page 4 6:4. https://doi.org/10.3390/JMMP6010004

16. Alifui-Segbaya F, Ituarte IF, Hasanov S, et al (2023) Opportunities and Limitations of Additive Manufacturing. Springer Handbooks Part F1592:125–143. https://doi.org/10.1007/978-3-031-20752-5_9

17. Alkunte S, Fidan I (2023) Machine Learning-Based Fatigue Life Prediction of Functionally Graded Materials Using Material Extrusion Technology. Journal of Composites Science 2023, Vol 7, Page 420 7:420. https://doi.org/10.3390/JCS7100420

18. Fidan I, Imeri A, Gupta A, et al (2019) The trends and challenges of fiber reinforced additive manufacturing. International Journal of Advanced Manufacturing Technology 102:1801–1818. https://doi.org/10.1007/S00170-018-03269-7

19. Hasanov S, Gupta A, Nasirov A, Fidan I (2020) Mechanical characterization of functionally graded materials produced by the fused filament fabrication process. J Manuf Process 58:923–935. https://doi.org/10.1016/J.JMAPRO.2020.09.011

20. Hasanov S, Gupta A, Alifui-Segbaya F, Fidan I (2021) Hierarchical homogenization and experimental evaluation of functionally graded materials manufactured by the fused filament

fabrication process. Compos Struct 275:114488. https://doi.org/10.1016/J.COMPSTRUCT.2021.114488

21. Anand Kumar S, Shivraj Narayan Y (2019) Tensile Testing and Evaluation of 3D-Printed PLA Specimens as per ASTM D638 Type IV Standard. Lecture Notes in Mechanical Engineering 79–95. https://doi.org/10.1007/978-981-13-2718-6_9

22. Fidan I, Russell N, Imeri A, et al (2020) Investigation of the Tensile Properties in Fiber-Reinforced Additive Manufacturing and Fused Filament Fabrication. International Journal of Rapid Manufacturing 9:. https://doi.org/10.1504/ijrapidm.2020.10019313

23. Vidakis N, Petousis M, Mountakis N, et al (2023) Energy Consumption vs. Tensile Strength of Poly[methyl methacrylate] in Material Extrusion 3D Printing: The Impact of Six Control Settings. Polymers (Basel) 15:. https://doi.org/10.3390/polym15040845

24. Ghahramani P, Behdinan K, Moradi-Dastjerdi R, Naguib HE (2021) Theoretical and experimental investigation of MWCNT dispersion effect on the elastic modulus of flexible PDMS/MWCNT nanocomposites. Nanotechnol Rev 11:. https://doi.org/10.1515/ntrev-2022-0006